A *k*-space Green's function solution for acoustic initial value problems in homogeneous media with power law absorption

Bradley E. Treeby[a] and B. T. Cox
Department of Medical Physics and Bioengineering, University College London, Gower Street, London, WC1E 6BT, United Kingdom

(Received 25 October 2010; revised 27 March 2011; accepted 30 March 2011)

An efficient Green's function solution for acoustic initial value problems in homogeneous media with power law absorption is derived. The solution is based on the homogeneous wave equation for lossless media with two additional terms. These terms are dependent on the fractional Laplacian and separately account for power law absorption and dispersion. Given initial conditions for the pressure and its temporal derivative, the solution allows the pressure field for any time $t > 0$ to be calculated in a single step using the Fourier transform and an exact *k*-space time propagator. For regularly spaced Cartesian grids, the former can be computed efficiently using the fast Fourier transform. Because no time stepping is required, the solution facilitates the efficient computation of the pressure field in one, two, or three dimensions without stability constraints. Several computational aspects of the solution are discussed, including the effect of using a truncated Fourier series to represent discrete initial conditions, the use of smoothing, and the properties of the encapsulated absorption and dispersion. © *2011 Acoustical Society of America*. [DOI: 10.1121/1.3583537]

PACS number(s): 43.35.Bf, 43.20.Bi, 43.20.Hq, 43.80.Cs [TDM] Pages: 3652–3660

I. INTRODUCTION

There are many applications in acoustics in which the absorption over the frequency range of interest follows a frequency power law. For example, the absorption in soft biological tissue over diagnostic ultrasound frequencies follows a frequency power law in which the exponent is between 1 and 2.[1] Similarly, the absorption in marine sediments follows a power law where the exponent is close to 1.[2] Classical viscous loss terms such as that used in Stokes' wave equation are not sufficiently general to account for power law absorption with arbitrary frequency dependence.[3] Consequently, there has been a focus on deriving new wave equations which facilitate this generality. These equations are typically based on the inclusion of a fractional derivative operator. In the case of a linear homogeneous medium, this gives an equation of the form[4]

$$\left(\nabla^2 - \frac{1}{c_0^2}\frac{\partial^2}{\partial t^2} + \tau\Pi\right) p(\mathbf{r}, t) = 0. \tag{1}$$

Here p is the acoustic pressure at time t and position $\mathbf{r} \in \mathbb{R}^n$ where $n = 1, 2, 3$, c_0 is the sound speed, Π is a general derivative operator, and τ is a proportionality coefficient.

Szabo made the observation that the addition of a derivative operator of order y yields power law absorption with a $(y-1)$ frequency dependence.[5] Consequently, power law absorption with a non-integer frequency dependence can be modeled by using a derivative operator of fractional order. Several different operators have been proposed based on both the fractional temporal derivative[6–10] and the fractional Laplacian[4,11] (see Ref. 4 for a recent review). These equations represent various extensions of the Blackstock and Stokes equations to account for power law absorption of arbitrary order. It is the efficient solution of such equations that is the subject of interest here.

Both finite element and finite difference time domain solutions of wave equations based on the fractional temporal derivative have previously been discussed.[9,12,13] For governing equations of this type, the computation of the fractional temporal derivative requires the pressure time history at each grid node to be stored (such operators are calculated via convolution). For power law exponents close to 2, only a small number of previous terms are necessary. However, as the exponent approaches 1, this number increases rapidly, making this type of approach intractable for many three dimensional problems of interest. In the case of Fourier based *k*-space and pseudospectral time domain methods, it is possible to circumvent these memory effects by using a governing equation based on the fractional Laplacian rather than the fractional temporal derivative.[4] The computation of these operators requires the values of the pressure field at all other positions (rather than times) which are already inherently known.

Analytical time domain Green's functions have also recently been derived for a generalized lossy wave equation based on the fractional temporal derivative.[10] These solutions are based on dividing the Green's function into lossless and lossy components. The latter is then computed using stable law probability density functions.[14] However, for absorption with an arbitrary frequency dependence in the range 1 to 2, this requires the use of specialized functions and solution techniques. Other techniques for computing solutions in one dimension have also been proposed.[15,16] While useful for studying the effects of attenuation and dispersion on

[a]Author to whom correspondence should be addressed. Now at: College of Engineering and Computer Science, Australian National University, Canberra, ACT 0200, Australia. Electronic mail: bradley.treeby@anu.edu.au.

 0001-4966/2011/129(6)/3652/9/$30.00

different pulse shapes, these have not been extended to three dimensional problems.

Here, an exact Green's function solution to the absorbing wave equation proposed by Treeby and Cox[4] is derived. The governing equation is based on the fractional Laplacian and represents an extension of that given by Chen and Holm[11] to correctly account for sound speed dispersion. The derived solution is based on a lossy Green's function expressed in the spatial frequency domain or k-space. It allows the computation of the pressure field for any time $t > 0$ in a single step given initial conditions for the pressure and its temporal derivative. The solution method represents a generalization of that presented by Cox and Beard[17,18] for initial value problems in lossless media. The derivation of the Green's function solution is described in Sec. II and the corresponding numerical implementation is presented in Sec. III. Several computational aspects of the solution are discussed, including the effect of using a discretized computational domain and the properties of the encapsulated absorption and dispersion. Summary and discussion are then given in Sec. IV.

II. DERIVATION OF AN EXACT GREEN'S FUNCTION SOLUTION FOR THE ABSORBING WAVE EQUATION

A. Acoustic wave equation for power law absorption

For a homogeneous medium in which the acoustic absorption follows a frequency power law of the form

$$\alpha = \alpha_0 \omega^y. \tag{2}$$

The dispersive wave equation based on the fractional Laplacian is given by[4]

$$\left(\nabla^2 - \frac{1}{c_0^2}\frac{\partial^2}{\partial t^2} + \tau\frac{\partial}{\partial t}(-\nabla^2)^{y/2} + \eta(-\nabla^2)^{(y+1)/2}\right) \times p(\mathbf{r}, t) = 0. \tag{3}$$

Here α_0 is the absorption coefficient in Np $(\text{rad/s})^{-y}$ m^{-1}, ω is the angular frequency, y is the power law exponent, ∇^2 is the Laplacian, c_0 is the sound speed, $p(\mathbf{r}, t)$ is the acoustic pressure, and τ and η are proportionality coefficients given by

$$\tau = -2\alpha_0 c_0^{y-1}, \quad \eta = 2\alpha_0 c_0^y \tan(\pi y/2). \tag{4}$$

This equation is valid for power law exponents in the range $0 < y < 3$ for $y \neq 1$ under the smallness approximations $\alpha \ll \omega/c_p$ and $\eta\omega^{y-1}c_0^2/c_p^{y+1} \ll 1$, where c_p is the frequency dependent phase speed. The two additional derivative operators respectively account for power law absorption along with the corresponding dispersion (dependence of the sound speed on frequency) dictated by the Kramers-Kronig relations.[19]

B. Deriving the Green's function in k-space

Given initial conditions for $p(\mathbf{r}, t)$ and $\partial p(\mathbf{r}, t)/\partial t$, a solution to Eq. (3) for a homogeneous and unbounded medium can be formed using standard Green's function methods, where[20]

$$p(\mathbf{r}, t) = -\frac{1}{c_0^2}\int\left[p(\mathbf{r}_0, t_0)\frac{\partial g(\mathbf{r}, t|\mathbf{r}_0, t_0)}{\partial t_0} - g(\mathbf{r}, t|\mathbf{r}_0, t_0)\frac{\partial p(\mathbf{r}_0, t_0)}{\partial t_0}\right] d\mathbf{r}_0, \tag{5}$$

(here the integration is performed over $\mathbb{R}^n$). In this case, the Green's function $g(\mathbf{r}, t|\mathbf{r}_0, t_0)$ represents a solution to the equation

$$\left(\nabla^2 - \frac{1}{c_0^2}\frac{\partial^2}{\partial t^2} + \tau\frac{\partial}{\partial t}(-\nabla^2)^{y/2} + \eta(-\nabla^2)^{(y+1)/2}\right) \times g(\mathbf{r}, t|\mathbf{r}_0, t_0) = -\delta(\mathbf{r} - \mathbf{r}_0)\,\delta(t - t_0), \tag{6}$$

where δ is the Dirac delta function. Using the Fourier transform conventions defined in Ref. 21, the four dimensional Fourier transform over $\mathbf{r}$ and t is given by

$$\left(-k^2 + \frac{\omega^2}{c_0^2} - i\tau\omega k^y + \eta k^{y+1}\right) \mathrm{G}(\mathbf{k}, \omega|\mathbf{r}_0, t_0) = -\frac{1}{(2\pi)^4} e^{i\omega t_0} e^{-i\mathbf{k}\cdot\mathbf{r}_0}, \tag{7}$$

where $\mathbf{k}$ and ω are the spatial and temporal frequencies, respectively, the scalar wave number is given by $k^2 = \mathbf{k}\cdot\mathbf{k}$, and the Fourier transform of the fractional Laplacian is defined as

$$\mathbb{F}\left\{(-\nabla^2)^{y/2} f(\mathbf{r})\right\} = k^y \mathbb{F}\{f(\mathbf{r})\}, \tag{8}$$

(here $\mathbb{F}$ denotes the spatial Fourier transform). Solving for $\mathrm{G}(\mathbf{k}, \omega|\mathbf{r}_0, t_0)$ and then taking the inverse four dimensional Fourier transform yields an integral form of the required Green's function

$$g(\mathbf{r}, t|\mathbf{r}_0, t_0) = -\frac{c_0^2}{(2\pi)^4}\int\int h(\mathbf{k}, \omega) d\omega d\mathbf{k}, \tag{9}$$

where the integrand is given by

$$h(\mathbf{k}, \omega) = \frac{e^{-i\omega(t-t_0)} e^{i\mathbf{k}\cdot(\mathbf{r}-\mathbf{r}_0)}}{\omega^2 - i\tau c_0^2\omega k^y + \eta c_0^2 k^{y+1} - (c_0 k)^2}. \tag{10}$$

This expression for the Green's function is not yet computationally useful due to the singularities in the integrand. Following the approach taken by Jackson for lossless media,[20] these singularities can be removed by analytically solving the integration with respect to ω (denoted herein as $\int d\omega$). For $t > t_0$, this can be achieved by integrating the complex function

$$f(\tilde{\xi}) = \frac{e^{-i\tilde{\xi}(t-t_0)}}{\tilde{\xi}^2 - i\tau c_0^2\tilde{\xi}k^y + \eta c_0^2 k^{y+1} - (c_0 k)^2}, \tag{11}$$

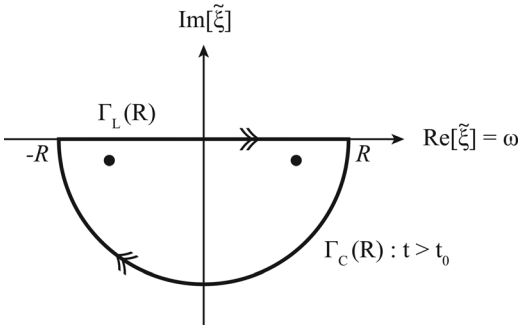

FIG. 1. Integration of the complex function $f(\tilde{\xi})$ over the contour $\Gamma_L(R) + \Gamma_C(R)$ using Cauchy's residue theorem. There are two poles located in the lower half plane.

over the contour $\Gamma(R) = \Gamma_L(R) + \Gamma_C(R)$ shown in Fig. 1, where $\tilde{\xi}$ is the extension of ω to the complex plane. The function $f(\tilde{\xi})$ has two poles located in the lower half of the complex plane

$$\tilde{\xi}_{p1},\ \tilde{\xi}_{p2} = \pm c_0 k \Upsilon - i\alpha_0 c_0^{y+1} k^y, \tag{12}$$

where Υ is defined as

$$\Upsilon = \sqrt{1 - \alpha_0^2 c_0^{2y} k^{2y-2} - 2\alpha_0 c_0^y k^{y-1} \tan(\pi y/2)}. \tag{13}$$

Setting $t_0 = 0$ without loss of generality (the function is invariant to temporal translations in t and t_0), by Cauchy's residue theorem the integration can be written as

$$\int_{-R}^{R} f(\tilde{\xi}) d\tilde{\xi} + \int_{\Gamma_C(R)} f(\tilde{\xi}) d\tilde{\xi} = -2\pi i \left(\mathrm{Res}\left\{ f(\tilde{\xi});\ \tilde{\xi}_{p1} \right\} + \mathrm{Res}\left\{ f(\tilde{\xi});\ \tilde{\xi}_{p2} \right\} \right), \tag{14}$$

where

$$\int d\omega = \lim_{R\to\infty} \left[\int_{-R}^{R} f(\tilde{\xi}) d\tilde{\xi} \right]. \tag{15}$$

The required residuals are given by

$$\mathrm{Res}\left\{ f(\tilde{\xi});\ \tilde{\xi}_{p1} \right\},\ \mathrm{Res}\left\{ f(\tilde{\xi});\ \tilde{\xi}_{p2} \right\} = \pm \frac{e^{-i(\pm c_0 k \Upsilon - i\alpha_0 c_0^{y+1} k^y)t}}{2 c_0 k \Upsilon}. \tag{16}$$

As $R \to \infty$, the integration around the contour $\int_{\Gamma_C(R)} f(\tilde{\xi}) d\tilde{\xi} \to 0$ and thus the solution for the analytical integration can be written as

$$\int d\omega = -2\pi i \left(\frac{e^{-\alpha_0 c_0^{y+1} k^y t}}{2 c_0 k \Upsilon} \right) \left(e^{-i c_0 k \Upsilon t} - e^{i c_0 k \Upsilon t} \right), = -2\pi \frac{\sin(c_0 k \Upsilon t) e^{-\alpha_0 c_0^{y+1} k^y t}}{c_0 k \Upsilon}, \tag{17}$$

where the second term has be simplified using the Euler identity $e^{i\theta} - e^{-i\theta} = 2i \sin\theta$. Note, for $t < t_0$, the contour integration shown in Fig. 1 is instead closed by a semi-circle in the upper half plane. As there are no poles located within the contour, the integrand is holomorphic and the Green's function is equal to zero. This demonstrates the causality of the governing equation given in Eq. (3) under the condition $\mathrm{Im}[\Upsilon] < \alpha_0 c_0^{y+1} k^y$.

Returning to Eq. (9), the required Green's function is now given by

$$g(\mathbf{r},\ t|\mathbf{r}_0,\ 0) = \frac{c_0^2}{(2\pi)^3} \int T_P(\mathbf{k},\ t)\, e^{i\mathbf{k}\cdot(\mathbf{r}-\mathbf{r}_0)} d\mathbf{k}, \tag{18}$$

where the time propagator $T_P(\mathbf{k},\ t)$ is defined as

$$T_P(\mathbf{k},\ t) = \frac{\sin(c_0 k \Upsilon t)\, e^{-\alpha_0 c_0^{y+1} k^y t}}{c_0 k \Upsilon}. \tag{19}$$

The corresponding temporal derivative of the Green's function can be written as

$$\frac{\partial g(\mathbf{r},\ t|\mathbf{r}_0,\ 0)}{\partial t} = \frac{c_0^2}{(2\pi)^3} \int \hat{T}_P(\mathbf{k},\ t)\, e^{i\mathbf{k}\cdot(\mathbf{r}-\mathbf{r}_0)} d\mathbf{k}, \tag{20}$$

where the gradient time propagator $\hat{T}_P(\mathbf{k},\ t)$ is defined as

$$\hat{T}_P(\mathbf{k},\ t) = e^{-\alpha_0 c_0^{y+1} k^y t} \times \left[\cos(c_0 k \Upsilon t) - \frac{\alpha_0 c_0^y k^{y-1} \sin(c_0 k \Upsilon t)}{\Upsilon} \right]. \tag{21}$$

If $\alpha_0 = 0$, i.e., the medium is lossless, $\Upsilon = 1$ and the two time propagators reduce to

$$T_P(\mathbf{k},\ t) = \frac{\sin(c_0 k t)}{c_0 k}, \quad \hat{T}_P(\mathbf{k},\ t) = \cos(c_0 k t). \tag{22}$$

For lossless media, a Green's function of this form can also be derived by taking the Fourier transform of the free space Green's function and then simplifying using the spherically symmetric part of the corresponding spherical harmonic expansion.[22]

C. Green's function solution for the initial value problem

Equations (18)–(21) can now be combined with Eq. (5) using the result $\partial g/\partial t_0 = -\partial g/\partial t$ (due to the temporal translational invariance of the Green's function) to give

$$p(\mathbf{r},\ t) = \frac{1}{(2\pi)^3} \int\int \left[p(\mathbf{r}_0,\ 0)\, \hat{T}_P + \frac{\partial p(\mathbf{r}_0,\ 0)}{\partial t} T_P \right] \times e^{i\mathbf{k}\cdot(\mathbf{r}-\mathbf{r}_0)} d\mathbf{k} d\mathbf{r}_0. \tag{23}$$

This equation is an exact solution to Eq. (3) for the acoustic pressure at any time $t > 0$ given initial conditions for the pressure and its temporal derivative. The required integrals

may be calculated sequentially and written succinctly using the Fourier transform

$$p(\mathbf{r}, t) = \mathbb{F}^{-1}\left\{ \mathbb{F}\{p(\mathbf{r}_0, 0)\}\, \hat{T}_P + \mathbb{F}\left\{ \frac{\partial p(\mathbf{r}_0, 0)}{\partial t} \right\} T_P \right\}, \quad (24)$$

where $\mathbb{F}$ and $\mathbb{F}^{-1}$ represent the forward and inverse spatial Fourier transforms, respectively, and the expression is valid in one, two, and three dimensions. A solution of this form for lossless media was previously presented by Cox and Beard to model initial value problems in photoacoustics in which $\partial p(\mathbf{r}, 0)/\partial t = 0$.[17,18] This was later extended to account for acoustic absorption with linear frequency dependence but no dispersion.[23] Because the solution is computed by transforming to and from the spatial frequency domain, there are obvious analogies to other spectral techniques, including k-space,[22] pseudospectral time domain,[24] and angular spectrum methods.[25] In the lossless case, the solution can also be related to exact nonstandard finite difference methods[26] which form the basis for other k-space techniques.[27]

III. NUMERICAL IMPLEMENTATION

A. Discrete solution

The numerical implementation of Eq. (24) can be achieved as follows. Given initial conditions compactly supported within a computational domain $\Omega \subset \mathbb{R}^n$ in n-dimensional space, the first step is to discretize Ω. The use of a regularly spaced Cartesian grid allows the Fourier transform to be computed efficiently using the fast Fourier transform (FFT). The values for the initial conditions at each of the grid nodes are then assigned. Next, an n-dimensional plaid wavenumber matrix k is created based on the properties of Ω.[28] The pressure within the domain at some time $t > 0$ can then be computed using the forward and inverse FFT via Eq. (24) using the coefficients defined in Eqs. (13), (19), and (21). If the temporal evolution of the pressure field is required, only one additional inverse FFT is needed for each additional value of t. Note, the use of the FFT to compute the discrete solution of Eq. (24) implicitly assumes the pressure field is periodic in space. Consequently, waves leaving the computational domain on one side will reappear on the opposite side. For the examples given here, the size of the computational grid was extended to avoid these effects.

B. Discrete initial conditions and oscillations

The application of Eq. (24) for particular discrete initial conditions can result in oscillations in the numerical solution for the pressure field that are not intuitively expected. These oscillations are also encountered in other spectral methods and occur because the discretization of the computational domain causes the corresponding Fourier space to become discrete and bounded (i.e., there is only a finite number of spatial wavenumbers the computational grid can support).[29] In this case, a discrete spatial delta function can be considered as the discrete sampling of a continuous function derived from a truncated Fourier series with the corresponding finite number of expansion coefficients (this function is often referred to as the band-limited interpolant).[29]

In general, any discrete initial conditions for p and $\partial p/\partial t$ can be decomposed into a weighted sum of discrete spatial delta functions located at the grid nodes. Consequently, a more detailed understanding of the origins of these oscillations can be derived from studying the response of the numerical solution to a single discrete delta function located at one of the nodes. For example, consider the one-dimensional lossless problem in which $\partial p(x, 0)/\partial t = 0$ and the initial pressure $p(x, 0) \equiv p_0(x)$ is given by a discrete spatial delta function

$$p_0(x_n) = \begin{cases} 1, & n = 0 \\ 0, & n \neq 0 \end{cases} \quad (25)$$

(here $x_n = n\Delta x$ for $n \in \mathbb{Z}$). In this case, Eq. (24) reduces to

$$p(x_n, t) = \mathbb{F}^{-1}\{\mathbb{F}\{p_0(x_n)\}\, \cos(c_0 k_m t)\}, \quad (26)$$

where $k_m = m\Delta k$ for $m \in \mathbb{Z}$. The discrete Fourier transform of $p_0(x_n)$ can be written explicitly as

$$\mathrm{P}_0(k_m) = \sum_{n=-N/2}^{N/2-1} p_0(x_n) e^{\frac{2\pi i}{N} mn}, \quad (27)$$

where the number of grid nodes N is taken to be even, and $\Delta x \Delta k = 2\pi/N$. For the initial conditions given by Eq. (25), the Fourier expansion coefficients are given simply by $\mathrm{P}_0(k_m) = 1, \forall m$. The corresponding continuous function $\hat{p}_0(x)$ derived from the finite set of expansion coefficients (i.e., the band-limited interpolant) is then given by[30]

$$\begin{aligned} \hat{p}_0(x) &= \frac{1}{N} \sum_{m=-N/2}^{N/2-1} \mathrm{P}_0(k_m) e^{-\frac{2\pi i}{N} \frac{mx}{\Delta x}} \\ &= \frac{1}{N} [i + \cot(x\pi/\Delta x N)]\, \sin(x\pi/\Delta x), \end{aligned} \quad (28)$$

where the limit of $\hat{p}_0(x)$ as $x \to 0$ is equal to 1. The discrete initial pressure given by Eq. (25) can then be obtained by sampling $\hat{p}_0(x)$ at $x = n\Delta x$. The discrete source function $p_0(x_n)$ and the corresponding band-limited interpolant $\hat{p}_0(x)$ are shown in the upper panel of Fig. 2. The oscillations in $\hat{p}_0(x)$ arise because the function is derived from the summation of a finite number of sinusoids. Their appearance can thus be considered analogous to Gibbs' phenomenon.

A solution for $p(x, t)$ for $\partial p(x, 0)/\partial t = 0$ and $p(x, 0) = \hat{p}_0(x)$ can now be written as a function of the band-limited interpolant

$$p(x, t) = \frac{1}{2}\hat{p}_0(x - tc_0) + \frac{1}{2}\hat{p}_0(x + tc_0). \quad (29)$$

This expression allows the origin of the oscillations in the pressure field calculated by Eq. (26) to be easily explained. If $t = l\Delta x/c_0$ and l is an integer, the band-limited interpolant $\hat{p}_0(x)$ will be translated by an integer multiple of the grid spacing. Consequently, if $p(x, t)$ is sampled at $x = n\Delta x$, the

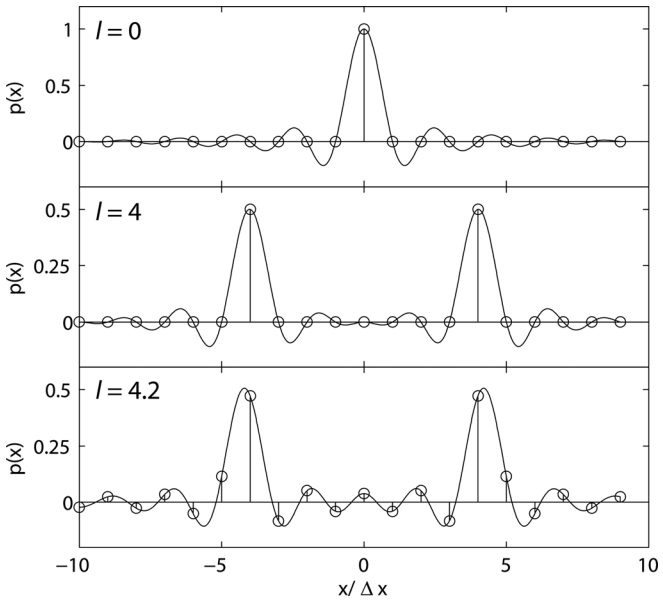

FIG. 2. Propagation of a discrete spatial delta function in one dimension. The discrete pressure is shown as a stem plot with the corresponding band-limited interpolant shown as a solid line (top panel). If $t = l\Delta x/c_0$ and l is not an integer, the band-limited interpolant is translated by an non-integer multiple of the grid spacing. This causes oscillations to appear in the discrete solution for the pressure field.

discrete solution for the pressure field will only depend on the values of $\hat{p}_0(x)$ at the grid nodes. As these values are equal to the discrete initial pressure, the shape of this distribution will be maintained. This is illustrated in the middle panel of Fig. 2 where $l = 4$. The discrete pressure field is shown as a stem plot with the continuous pressure field $p(x, t)$ overlaid as a solid line. In this case, the solution is given as two discrete spatial delta functions of half the original magnitude as expected.

Conversely, if l is not an integer, the band-limited interpolant $\hat{p}_0(x)$ will be translated by an non-integer multiple of the grid spacing. If $p(x, t)$ is sampled at $x = n\Delta x$, the solution will depend on values of $\hat{p}_0(x)$ in between the grid nodes (i.e., at $x \neq n\Delta x$). Because the function $\hat{p}_0(x)$ is oscillatory between the grid nodes, oscillations in the pressure field will also arise. This is illustrated in the lower panel of Fig. 2 where $l = 4.2$. In this case, the discrete solution for the pressure field (shown by the stem plot) now contains oscillations. For generalized initial conditions, the equivalent response can be obtained by superposition.

Note, the interpolation function given by Eq. (28) has both real and imaginary components, however, the latter is always exactly zero at the grid nodes. As the pressure is a real quantity, it is assumed that the required pressure field corresponds to the real part of the obtained solution and only these parts are plotted. It is also possible to avoid the complex part by splitting the end limits of the summation.[30]

C. Smoothing the initial conditions

In higher dimensions, oscillations will always appear within the calculated pressure field when the initial pressure is given by a discrete spatial delta function. This is because, for a regularly spaced grid, the time taken to travel horizontally or vertically between the grid nodes will be different from the time to travel diagonally. As a result, the discrete solution will always depend on values of the underlying band-limited interpolant at positions where it is oscillatory. As discussed in the previous section, the occurrence of these oscillations is deterministic and an intrinsic property of the discretization of the computational domain. However, in some situations a practical method of reducing the visible oscillations may be desirable. For example, in many cases the discrete initial conditions represent an approximation to a continuous function for which the analogous pressure field does not contain any oscillations.

The oscillations can be reduced by changing the characteristics of the band-limited interpolant by applying a window in the spatial frequency domain. This modifies the properties of the bounded Fourier space by forcing the expansion coefficients to decay. Selecting the most appropriate window requires a trade off between maintaining an acceptable main lobe width (which affects the amount of smoothing) whilst minimizing the side lobe levels (which affects the observable oscillations). Note, the rectangular window is equivalent to the unwindowed case and produces the smallest possible main lobe width.

Figure 3 illustrates the initial pressure distribution, recorded time series, and the corresponding amplitude spectrum for the propagation of a spatial impulse in one dimension. Here, $N_x = 256$, $\Delta x = 0.05 \times 10^{-3}$ m, and $c_0 = 1500$ m s^{-1} (supporting a maximum frequency of 15 MHz), $\Delta t = 1 \times 10^{-9}$ s, and the source and receiver are positioned are 3×10^{-3} m apart. The top row is for the unwindowed case. The middle and lower panels of Fig. 3 show the same example with the initial pressure smoothed using frequency domain Hanning and Blackman windows, respectively. The magnitudes of the smoothed initial pressure distributions have been corrected by the corresponding coherent gain of the windows. The Blackman window has a lower side lobe level and thus the oscillations in the recorded time series are less apparent. However, it also has a larger main lobe width and thus the spatial delta function appears more heavily smoothed. Both windows have high side-lobe roll-off rates so the oscillations decay quickly away from the peak. A large number of other variations are also possible by choosing from the families of existing window functions. For minimizing oscillations, the Blackman family of windows is a good choice. Note, the application of the Hanning window produces the three point optimum source pattern discussed by Lin and Thylén.[31] Similarly, the application of the Cosine window is analogous to the corresponding two point optimum source pattern.[31,32]

D. Absorption and dispersion

To demonstrate the characteristics of the acoustic absorption and dispersion encapsulated by Eq. (24), the propagation of a spatial delta function smoothed back a Blackman window through a one dimensional homogeneous medium was investigated. The absorption and dispersion were extracted from the time series recorded at two points where $N_x = 2048$, $\Delta x = 12.8 \times 10^{-3}$ m, $c_0 = 1500$ m s^{-1},

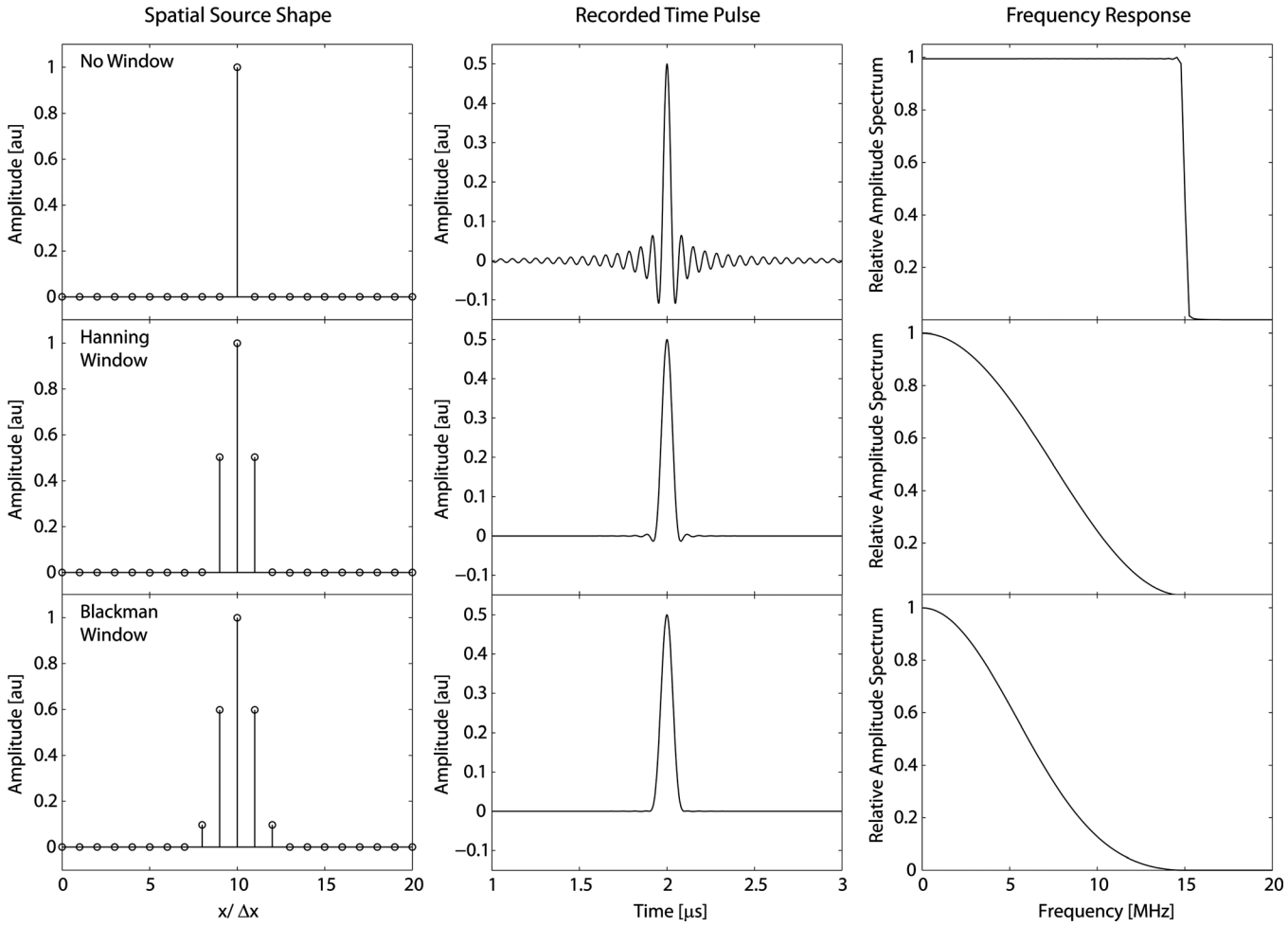

FIG. 3. Propagation of a spatial delta function in one dimension. The pressure field is sampled with a high temporal resolution at a single position 3×10^{-3} m from the source. The resulting time series displays significant oscillations. These can be mitigated by windowing the source distribution. The main lobe width of the window affects the amount of smoothing, while the side lobe level affects the amount of observable oscillations. The effect of two windowing functions on the initial source shape, recorded time history, and frequency content of the propagated wave is illustrated.

and $\Delta t = 1 \times 10^{-9}$ s.[4] The extracted parameters are shown in Figs. 4(a) and 4(b) with open circles. The solid lines show the theoretical comparisons derived from Eq. (2) and the corresponding Kramers-Kronig relation.[19] The three curves correspond to absorption values of $\alpha_{0,\mathrm{dB}} = 0.1$ and $y = 1.9$ (equivalent to $\alpha_0 = 1.40 \times 10^{-13}$), $\alpha_{0,\mathrm{dB}} = 0.25$ and $y = 1.5$ (equivalent to $\alpha_0 = 1.83 \times 10^{-10}$), and $\alpha_{0,\mathrm{dB}} = 0.5$ and $y = 1.1$ (equivalent to $\alpha_0 = 1.91 \times 10^{-7}$). Here $\alpha_{0,\mathrm{dB}}$ is given in units of dB MHz^{-y} cm^{-1} and α_0 in units of Np $(\mathrm{rad/s})^{-y}$ m^{-1}. For the range of absorption values displayed, there is a very good agreement between the theoretical values of absorption and dispersion and those exhibited by the model.

At high frequencies and high values of the absorption parameters, the smallness approximations under which the lossy terms are derived are no longer valid. Consequently, the absorption operator will have an unintended second order effect on the dispersion (and vice versa for the dispersion operator). This is illustrated in Figs. 4(c) and 4(d). The two curves correspond to absorption values of $\alpha_{0,\mathrm{dB}} = 0.25$ and $y = 2$ (equivalent to $\alpha_0 = 7.29 \times 10^{-14}$), and $\alpha_{0,\mathrm{dB}} = 1$ and $y = 1.5$ (equivalent to $\alpha_0 = 7.31 \times 10^{-10}$). Although the absorption for $y = 2$ should be non-dispersive, for high values of ω and α_0, a small perturbation is introduced. As the corresponding dispersion term is zero for $y = 2$, there is no equivalent second order modification to the encapsulated absorption and this remains exact. For $y = 1.5$, a perturbation to both the absorption and dispersion is seen. However, the high values of frequency and absorption (in this case more than 200 dB cm^{-1}) at which these effects become noticeable means that they will be negligible for most simulations of most practical interest.

E. Numerical example

To illustrate the capabilities of the developed numerical solution, a simple example of an initial value problem in two dimensions is given (see Fig. 5). Initial value problems of this kind can arise in many areas of acoustics in which the time scale over which the acoustic source is applied is much shorter than the time scale of interest for the acoustic propagation. There are several mechanisms by which such a source may be produced, for example mechanical or flow induced vibration, magnetic induction, or electromagnetic absorption. These mechanisms may act as a pressure source, or may move the fluid directly (changing the particle velocity and

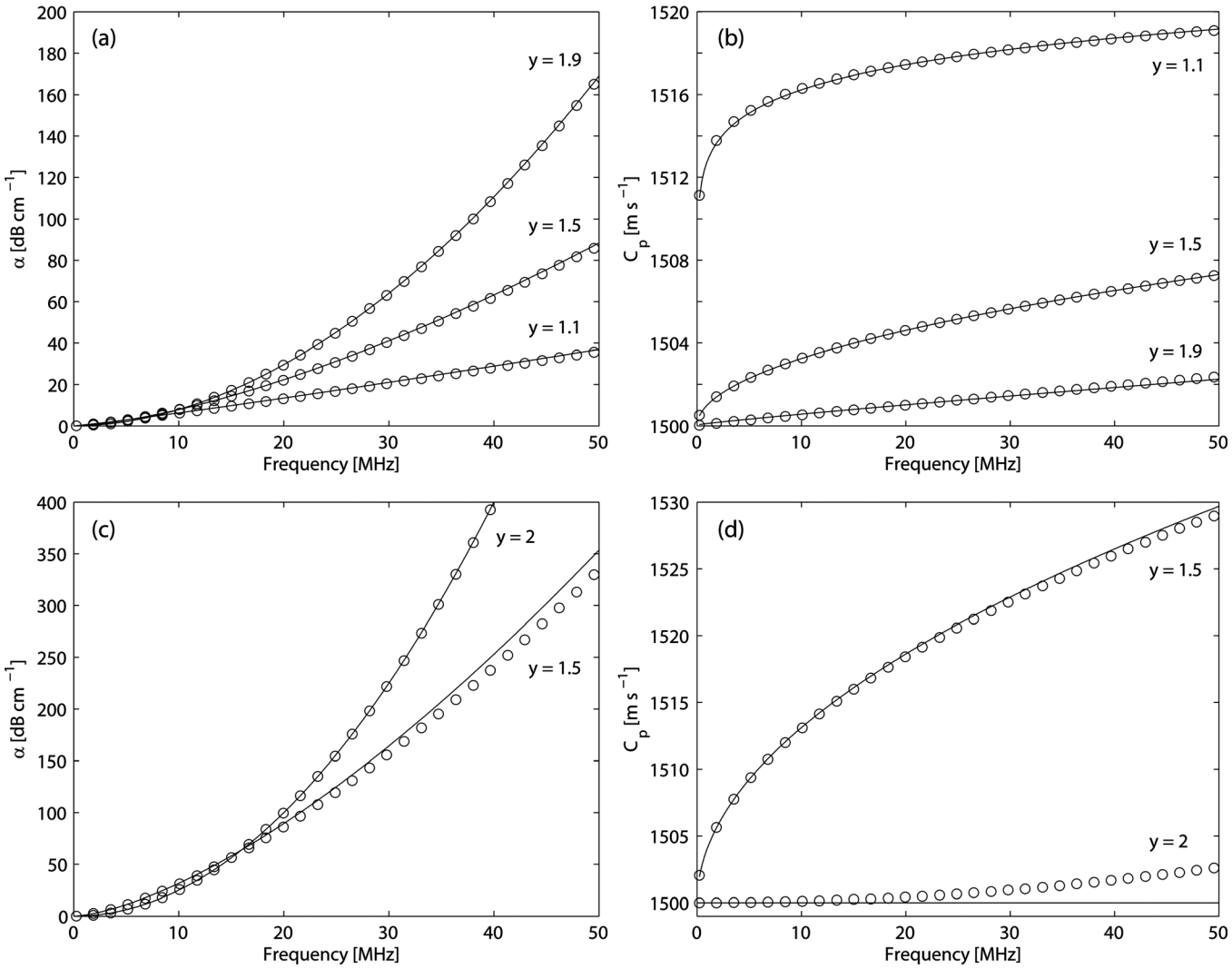

FIG. 4. Properties of the (a) absorption and (b) dispersion encapsulated by Eq. (24). The three curves correspond to absorption parameters of $\alpha_{0,\mathrm{dB}} = 0.1$ and $y = 1.9$, $\alpha_{0,\mathrm{dB}} = 0.25$ and $y = 1.5$, and $\alpha_{0,\mathrm{dB}} = 0.5$ and $y = 1.1$. Analytical values are shown as a solid line for comparison. (c) and (d) At high values of ω and α_0, second order effects become noticeable.

thus producing a pressure gradient). Here, the utilized source function was chosen to be two circular disks of radius $4\Delta x$ and $3\Delta x$ with corresponding amplitudes of 4 and 3. Practically, for the case of an initial pressure distribution, this could correspond to a photoacoustic source produced by two disk-shaped optical absorbers, however, any other source distribution could equally be used. The source function was smoothed using a 2D Blackman window and the simulation parameters were given by N_x and $N_z = 64$, Δx and $\Delta z = 0.1 \times 10^{-3}$ m, $c_0 = 1500$ m s^{-1}, $\alpha_{0,\mathrm{dB}} = 0.75$ dB MHz^{-y} cm^{-1} and $y = 1.5$ (equivalent to $\alpha_0 = 5.48 \times 10^{-10}$ Np (rad/s)$^{-y}$ m^{-1}).

The left column of Fig. 5 shows the pressure field obtained by assigning the source function to $p(\mathbf{r}, 0)$ with $\partial p(\mathbf{r}, 0)/\partial t = 0$ for t = 0, 250, 500, and 1000 ns. Because no time stepping is required, these results are obtained directly via Eq. (24). Moreover, for the same source condition, only one additional inverse FFT is required to compute the pressure field at each additional time point. The central column shows the equivalent results obtained by assigning the source function (scaled by 5×10^6) to $\partial p(\mathbf{r}, 0)/\partial t$ with $p(\mathbf{r}, 0) = 0$, and the right column by assigning the source function to both $p(\mathbf{r}, 0)$ and $\partial p(\mathbf{r}, 0)/\partial t$.

Note, the small grid size used in this example was chosen to generate images suitable for display (the complete example took less than a second to run using MATLAB on a standard workstation). As the solution relies only on the efficiency of the FFT, it is straightforward to run simulations with dense computational grids, including in three dimensions. For example, a simulation using a three dimensional grid with $128 \times 128 \times 128$ voxels evaluated at 100 different time values took around forty seconds to compute on the same workstation. The FFT has also been shown to perform well when computed using graphics processing units (GPUs) which provides a convenient mechanism for parallelization.[28]

IV. SUMMARY AND DISCUSSION

An efficient Green's function solution for initial value problems in homogeneous media with power law absorption has been derived. This allows the pressure field for any time $t > 0$ to be computed given initial conditions for the pressure

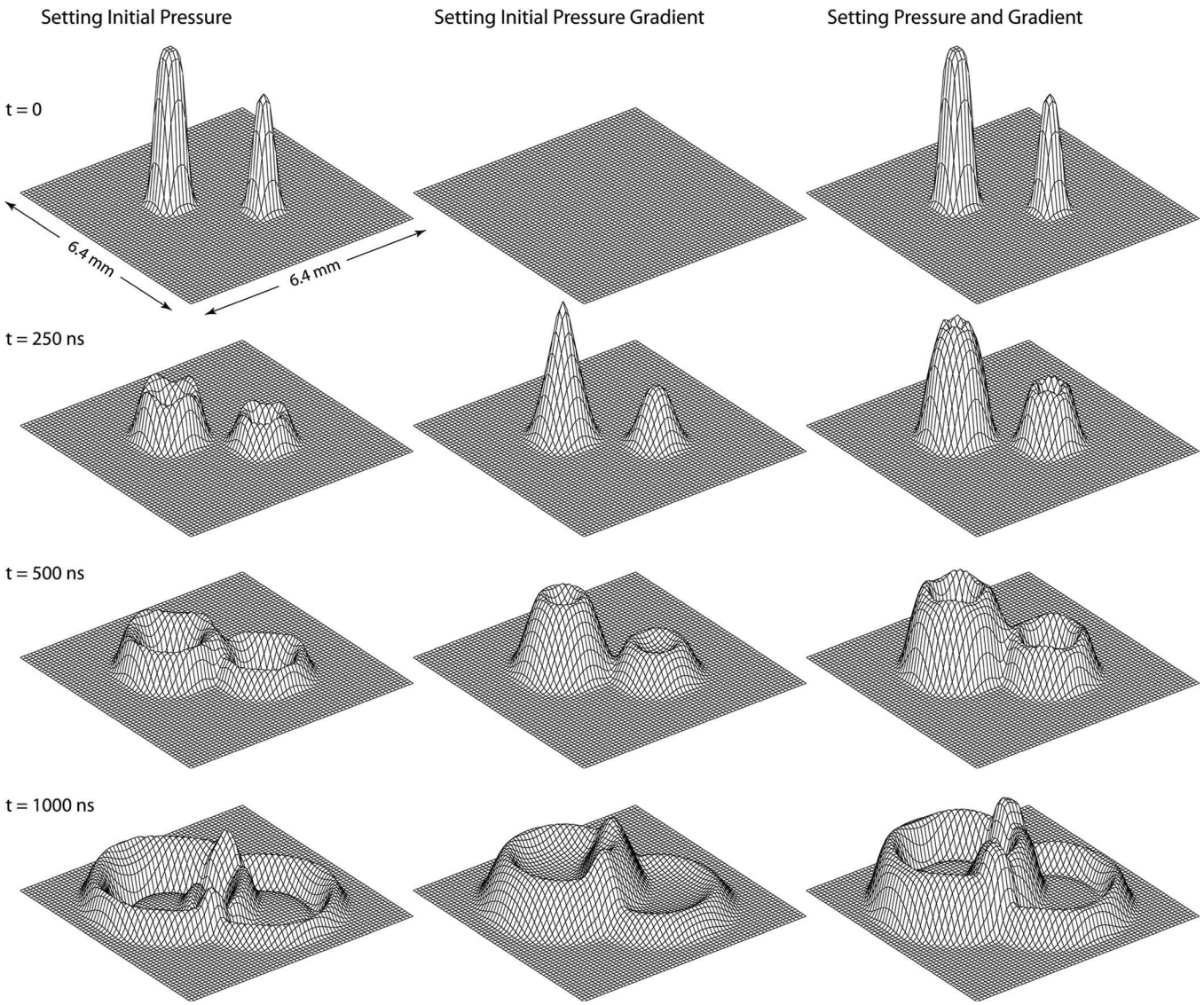

FIG. 5. Simulation of the pressure field within a two dimensional domain using a source function given by two circular disks smoothed using a Blackman window. The left column shows the pressure field obtained by assigning the source function to the initial pressure with the gradient set to zero. The central column shows the equivalent results obtained by assigning the source function to the initial pressure gradient with the pressure set to zero. The right column shows the analogous results obtained by setting both initial conditions.

and its temporal derivative. The solution is obtained in a single step using the Fourier transform and a k-space time propagator. For regularly spaced Cartesian grids, the former can be computed efficiently using the FFT. Because no time stepping is required, this provides an efficient method for calculating the pressure field in one, two, or three dimensions without stability constraints. The numerical implementation of the solution has also been discussed, including the use of source smoothing to avoid oscillations arising from the discretization of the computational domain.

The derived solution is based on the fractional Laplacian wave equation and is exact in continuous form. This governing equation encapsulates power law absorption and dispersion under the smallness approximations described in Sec. II.B. Considering the strength of typical acoustic sources, the fidelity of acoustic measurement systems, and the range of absorption values normally encountered, in practice these smallness approximations will almost always be satisfied. Compared to the pseudospectral time domain model discussed in Ref. 4 (based on the same governing equation), the Green's function solution accurately encapsulates the absorption and dispersion characteristics without additional numerical errors.

In comparison to other finite difference or finite element solutions of absorbing wave equations discussed in the literature, the Green's function solution developed here has several advantages. First, because the gradients are effectively calculated spectrally, only two points per wavelength are required. This provides a significant reduction in the size of the required computational grid, particularly for three dimensional problems. Second, because the governing equation is based on the fractional Laplacian, no temporal history of the pressure field is needed. Third, there are no imposed stability constraints and thus the pressure field can be evaluated only at the specific times required. Overall, this allows the pressure field to be computed very efficiently. On the other hand,

the solution presented here is restricted to a homogeneous domain. Similarly, the utilized Green's function approach cannot be extended to model nonlinear wave propagation.

While applicable to many areas of acoustics, the developed solution has particular relevance to the efficient simulation of short acoustic pulses through soft biological tissue. For example, in the field of biomedical photoacoustics, similar models for lossless media have been used as part of iterative approaches to extract quantitative tissue information.[33] In this case, accurately accounting for acoustic absorption is of critical importance as errors in the magnitude of the modeled pressure directly manifest as errors in the estimation of the tissue properties.[34]

ACKNOWLEDGMENTS

This work was supported by the Engineering and Physical Sciences Research Council, UK. The authors would like to thank Nick Ovenden for useful discussion on complex analysis.

[1]J. C. Bamber, " Attenuation and Absorption," in *Physical Principles of Medical Ultrasonics*, edited by C. R. Hill, J. C. Bamber, and G. R. ter Haar (John Wiley, Chichester, 2004), pp. 93–166.
[2]M. J. Buckingham, "Theory of acoustic attenuation, dispersion, and pulse propagation in unconsolidated granular materials including marine sediments," J. Acoust. Soc. Am. **102**, 2579–2596 (1997).
[3]M. J. Buckingham, "Causality, Stokes' wave equation, and acoustic pulse propagation in a viscous fluid," Phys. Rev. E **72**, 026610 (2005).
[4]B. E. Treeby and B. T. Cox, "Modeling power law absorption and dispersion for acoustic propagation using the fractional Laplacian," J. Acoust. Soc. Am. **127**, 2741–2748 (2010).
[5]T. L. Szabo, "Time domain wave equations for lossy media obeying a frequency power law," J. Acoust. Soc. Am. **96**, 491–500 (1994).
[6]M. Caputo, "Linear models of dissipation whose Q is almost frequency independent-II," Geophys. J. Int. **13**, 529–539 (1967).
[7]W. Chen and S. Holm, "Modified Szabo's wave equation models for lossy media obeying frequency power law," J. Acoust. Soc. Am. **114**, 2570–2574 (2003).
[8]M. Liebler, S. Ginter, T. Dreyer, and R. E. Riedlinger, "Full wave modeling of therapeutic ultrasound: Efficient time-domain implementation of the frequency power-law attenuation," J. Acoust. Soc. Am. **116**, 2742–2750 (2004).
[9]M. G. Wismer, "Finite element analysis of broadband acoustic pulses through inhomogenous media with power law attenuation," J. Acoust. Soc. Am. **120**, 3493–3502 (2006).
[10]J. F. Kelly, R. J. McGough, and M. M. Meerschaert, "Analytical time-domain Green's functions for power-law media," J. Acoust. Soc. Am. **124**, 2861–2872 (2008).
[11]W. Chen and S. Holm, "Fractional Laplacian time-space models for linear and nonlinear lossy media exhibiting arbitrary frequency power-law dependency," J. Acoust. Soc. Am. **115**, 1424–1430 (2004).
[12]G. V. Norton and J. C. Novarini, "Including dispersion and attenuation directly in the time domain for wave propagation in isotropic media," J. Acoust. Soc. Am. **113**, 3024–3031 (2003).
[13]G. V. Norton and J. C. Novarini, "Including dispersion and attenuation in time domain modelling of pulse propagation in spatially-varying media," J. Comput. Acoust. **12**, 501–519 (2004).
[14]V. M. Zolotarev, *One-dimensional Stable Distributions* (American Mathematical Society, Providence, 1986), pp. 1–261.
[15]T. L. Szabo, "The material impulse response for broadband pulses in lossy media," in Proc. IEEE Ultrasonics Symp. **1**, 748–751.
[16]R. S. C. Cobbold, N. V. Sushilov, and A. C. Weathermon, "Transient propagation in media with classical or power-law loss," J. Acoust. Soc. Am. **116**, 3294–3303 (2004).
[17]B. T. Cox and P. C. Beard, "Fast calculation of pulsed photoacoustic fields in fluids using k-space methods," J. Acoust. Soc. Am. **117**, 3616–3627 (2005).
[18]B. T. Cox and P. C. Beard, "Modeling photoacoustic propagation in tissue using k-space techniques," in *Photoacoustic Imaging and Spectroscopy,* edited by L. V. Wang (CRC Press, Boca Raton, 2009), pp. 25–34.
[19]K. R. Waters, M. S. Hughes, J. Mobley, G. H. Brandenburger, and J. G. Miller, "On the applicability of Kramers-Kronig relations for ultrasonic attenuation obeying a frequency power law," J. Acoust. Soc. Am. **108**, 556–563 (2000).
[20]J. D. Jackson, *Classical Electrodynamics* (Wiley, New York, 1962), pp. 183–186.
[21]P. M. Morse and K. U. Ingard, *Theoretical Acoustics* (Princeton University Press, Princeton, 1968), p. 28.
[22]N. N. Bojarski, "The k-space formulation of the scattering problem in the time domain," J. Acoust. Soc. Am. **72**, 570–584 (1982).
[23]B. E. Treeby and B. T. Cox, "Fast, tissue-realistic models of photoacoustic wave propagation for homogeneous attenuating media," Proc. SPIE, **7177**, 717716 (2009).
[24]Q. H. Liu, "The pseudospectral time-domain (PSTD) algorithm for acoustic waves in absorptive media," IEEE Trans. Ultrason. Ferroelectr. Freq. Control **45**, 1044–1055 (1998).
[25]P. Stepanishen and K. Benjamin, "Forward and backward projection of acoustic fields using FFT methods," J. Acoust. Soc. Am. **71**, 803 (1982).
[26]R. E. Mickens, *Nonstandard Finite Difference Models of Differential Equations* (World Scientific, Singapore, 1994), pp. 166–192.
[27]T. D. Mast, L. P. Souriau, D. L. D. Liu, M. Tabei, A. I. Nachman, and R. C. Waag, "A k-space method for large-scale models of wave propagation in tissue," IEEE Trans. Ultrason. Ferroelectr. Freq. Control **48**, 341–354 (2001).
[28]B. E. Treeby and B. T. Cox, "k-Wave: MATLAB toolbox for the simulation and reconstruction of photoacoustic wave-fields," J. Biomed. Opt. **15**, 021314 (2010).
[29]L. Trefethen, *Spectral Methods in MATLAB* (Society for Industrial and Applied Mathematics, Philadelphia, 2000), pp. 9–27.
[30]J. S. Hesthaven, S. Gottlieb, and D. Gottlieb, *Spectral Methods for Time-Dependent Problems* (Cambridge University Press, Cambridge, 2007), pp. 24–28.
[31]Z. Lin and L. Thylén, "An analytical derivation of the optimum source patterns for the pseudospectral time-domain method," J. Comput. Phys. **228**, 7375–7387 (2009).
[32]T.-W. Lee and S. C. Hagness, "A compact wave source condition for the pseudospectral time-domain method," IEEE Antenn. Wireless Propag. Lett. **3**, 253–256 (2004).
[33]J. Laufer, B. Cox, E. Zhang, and P. Beard, "Quantitative determination of chromophore concentrations from 2D photoacoustic images using a nonlinear model-based inversion scheme," Appl. Opt. **49**, 1–15 (2010).
[34]B. E. Treeby, E. Z. Zhang, and B. T. Cox, "Photoacoustic tomography in absorbing acoustic media using time reversal," Inverse Probl. **26**, 115003 (2010).